# Looking at microbial metabolism by high-resolution $^2$H-NMR spectroscopy

We analyzed the applicability of high-resolution $^2$H-HMR spectroscopy for the analysis of microbe metabolism in samples of mitochondrion isolated from rat liver and from aqueous extracts of homogenates of rat liver and other organs and tissues in the presence of high $D_2O$ contents. Such analysis is possible due to the fast microbe adaptation to life in the heavy water. It is also shown that some enzymatic processes typical for the intact cells are preserved in the homogenized tissue preparations. The microbial and cellular metabolic processes can be differentiated via the strategic use of cell poisons and antibiotics.

1  **Looking at microbial metabolism by high-resolution $^{2}$H-NMR spectroscopy**

2

3  **Victor P. Kutyshenko,[1,*] Peter M. Beskaravayny,[1] Maxim V. Molchanov,[1] Svetlana I.**

4  **Paskevich[1], Dmitry A. Prokhorov,[1] and Vladimir N. Uversky[2,3,*]**

5

6  *[1]Institute of Theoretical and Experimental Biophysics Russian Academy of Sciences, 142290*

7  *Pushchino, Russia; [2]Institute for Biological Instrumentation, Russian Academy of Sciences,*

8  *142290 Pushchino, Moscow Region, Russia; Department of Molecular Medicine and USF*

9  *Health Byrd Alzheimer's Research Institute, College of Medicine, University of South*

10  *Florida, Tampa, Florida 33612, USA*

11

12  **Corresponding authors**: *To whom correspondence should be addressed: VNU, Department

13  of Molecular Medicine, University of South Florida, 12901 Bruce B. Downs Blvd., MDC07,

14  Tampa, Florida 33612, USA, Phone: 1-813-978-5816; Fax: 1-813-974-7357; E-mail:

15  vuversky@health.usf.edu; VPK, Institute of Theoretical and Experimental Biophysics of

16  Russian Academy of Science, 142290 Pushchino, Moscow region, Russia, e-mail:

17  kutyshenko@rambler.ru

18 **Abstract**

19 We analyzed the applicability of high-resolution $^2$H-HMR spectroscopy for the analysis of

20 microbe metabolism in samples of mitochondria isolated from rat liver and from aqueous

21 extracts of homogenates of rat liver in the presence of high $D_2O$ contents. Such analysis is

22 possible due to the fast microbe adaptation to life in the heavy water. It is also shown that

23 some enzymatic processes typical for the intact cells are preserved in the homogenized tissue

24 preparations. The microbial and cellular metabolic processes can be differentiated via the

25 strategic use of cell poisons and antibiotics.

26

27 **Key words**: Microbial metabolism; High resolution NMR; $^2$H-HMR spectroscopy; Heavy

28 water; Microbe adaptation;

## Introduction

Recent years witnessed an increased interest of researchers in the analysis of various biological fluids. This research is taken now as a fundamental basis of the metabolomics, which studies the metabolic profiles of animals and humans during their normal activity and at various pathological conditions, as well as looks at the effects of various drugs and other substances on specific organ/tissue, the whole organisms, and even on the entire ecosystem (Holmes, Wilson & Nicholson, 2008; Maher *et al.*, 2008; Nicholson & Lindon, 2008). Typically, term 'biological fluids' is taken as a synonym to 'body fluids' or 'biofluids' that correspond to liquids originating from inside the bodies of living people, such as urine, blood, saliva, sweat, cerebrospinal fluid, mucus, etc. However, this concept can be extended to include water washouts and aqueous extracts of the homogenates of various organs and tissues of animals (Kutyshenk*o et al.*, 2007; Kutyshenk*o et al.*, 2008a; Kutyshenk*o et al.*, 2008b) and plants (Molchano*v et al.*, 2012). Addition of these somewhat artificial biological fluids leads to the noticeable increase in the variability of experimental material suitable for comprehensive analysis and produces substantial information related not only to the organs under study, but also to the interactions of these organs with the remaining organism and with specific microorganisms.

The close connection between plants and animals with specific microorganisms constituting microbiomes or microbiotas is a well-established fact. In fact, animals, including humans, constantly coexist with microorganisms, being involved in numerous symbiotic interactions with various bacteria and yeast that densely populate intestines, skin, and tunica mucosa of airways, pharynx and urinary tract. Furthermore, some microorganisms can get access to various organs through bloodstream or other biofluids leading to the development of various pathologies. The current list of human symbiotic microorganisms includes ~5,000 species that are uniquely distributed between 15 and 18 sites of the permanent habitat in

54  males and females, respectively (Huma*n et al*., 2012a; Huma*n et al*., 2012b). Since different

55  organs are biochemically different, sets of symbiotic microorganisms populating them can

56  vary between different organs within the same organism. Many members of the human

57  microbiome are conditionally pathogenic microorganisms that can provoke development of

58  various maladies if appropriate conditions are given (Tancrede, 1992; Riabichenko &

59  Bondarenko, 2007; Y*u et al*., 2012). Under these circumstances, originally harmless and even

60  beneficiary symbiotic microorganisms can go bad and start negatively affect the normal

61  cellular and organ functions of the host organism, secreting specific toxins and ferments and

62  eventually leading to the metabolism distortion and cell death. Furthermore, by destroying the

63  host cells, microorganisms promote the release of the cell content into the extracellular

64  environment, thereby further exacerbating the course of a disease and negatively affecting the

65  overall condition of the host organism. In fact, sometimes, massive cell death can be a

66  self-propagating process, where proteins released from the dying cells affect neighboring

67  cells leading to their death and consequently generating favorable conditions for the

68  propagation of both the "own" symbiotic microorganisms of the microbiome and the

69  microorganisms introduced from the outside. Therefore, under such circumstances, therapy

70  should include both antibacterial and healing strategies.

71    In this work, the mitochondria suspension and the aqueous extracts from the liver

72  homogenates are used to model cell death and organ damage (necrosis) resulting from the

73  injuries and pathologies and to experimentally characterize the related processes. We propose

74  here an instrumental approach that can be used to detect and control both microbial and host

75  enzymatic processes taking place within the sites of disease origin. This approach is based on

76  the detection of the deuterium incorporation to the specific metabolism products. Here,

77  deuterium (in a form of heavy water) is added directly to the medium where the ferment

78  action and/or microorganism vital activity takes place. Our earlier analysis revealed that

79    many microorganisms can easily adapt to the conditions of high heavy water contents, and

80    presence of almost 100% heavy water does not significantly affect normal functioning of

81    certain microorganisms (Kushner, Baker & Dunstall, 1999; Molchano*v et al.*, 2012). Under

82    these conditions, deuterium can be incorporated to the substrates due to the existence of

83    efficient exchange between the protons of organic moieties of substrates and deuterium

84    present in media. Next, these deuterated substrates can be used in biochemical reactions

85    leading to the enzymatic incorporation of deuterium to the corresponding metabolism

86    products (Ewy, Ackerman & Balaban, 1988; Kushner, Baker & Dunstall, 1999; Budantsev,

87    Uversky & Kutyshenko, 2010; Molchano*v et al.*, 2012). One of the most informative

88    techniques to follow the mentioned processes in biological fluids is the high-resolution NMR

89    at the deuterium nuclei, 2H-NMR (Budantsev, Uversky & Kutyshenko, 2010). In comparison

90    with proton spectra, 2H-NMR spectra are characterized by lower resolution and lower

91    sensitivity. Furthermore, deuterium-deuterium couplings are about 40 times smaller than

92    proton-proton couplingsdeuterium-deuterium couplings. However, the overall shapes of

93    ^{1}H-NMR and ^{2}H-NMR spectra of organic components are rather similar. The only exception

94    here is the fact that due to the low spin-spin interaction constants, quadrupole broadening,

95    and the presence of various isotopomers, the multiplets seeing in the ^{1}H-NMR spectra are

96    typically presented by broad 'singlets' in the ^{2}H-NMR spectra (Emsley, Feeney & Sutcliffe,

97    1966). However, despite the aforementioned issues, 2H-NMR spectroscopy has numerous

98    advantages.

99        In this work, we show the applicability of the high-resolution ^{2}H-NMR spectroscopy for

100   the quantitative analysis of biological fluids using preparations of mitochondria suspension

101   and aqueous extracts from rat liver homogenates as illustrative example. It is important to

102   emphasize here that the proposed approach for studying microbial and host enzymatic

103   activities based on the analysis of deuterium incorporation to the metabolic products can be

104    of wide practical use in many other cases, when high $D_2O$ concentrations do not perturb the

105    physiological processes of the studied (Budantsev, Uversky & Kutyshenko, 2010).

106

107    **Materials and Methods**

108        Mitochondria were isolated from the livers of Wistar rats using the standard protocols

109    (Belosludtse*v et al*., 2009). Mitochondria samples used in our study were a generous gift of

110    Prof. Mironova G.D. The only modification of the isolation protocol in some preparations

111    was substitution of light water by heavy water (OOO Astrochim, Russia, 99.8%) done at our

112    request. The standard functional analysis revealed that the mitochondria isolated using such

113    modified heavy water-based protocol were active and preserved their activity for several

114    hours after isolation. Part of mitochondria isolated by a standard, light water-based approach

115    was subsequently treated with heavy water. The heavy water content in samples was

116    controlled using the characteristic features of 1H-NMR spectra. On average, the heavy water

117    content ranged from 40% to 57% in various samples prepared using the light water-based

118    approach and was higher than 86% in samples prepared by heavy water-based approach. The

119    freshly prepared samples had pH ~7.

120        Livers of the Vistar rats were a kind gift of Prof. Kichigina V.F. These animals were

121    sacrificed for the purpose of unrelated experiments (Popova, Sinelnikova & Kitchigina,

122    2008). Aqueous extracts of the rat liver homogenates were prepares using 0.40±0.03 g

123    samples which were first carefully homogenized in the eppendorfs using a special sterile

124    glass spatula and then diluted with 0.75 ml heavy water (CIL, USA, 99.9%). Samples were

125    centrifuged using the microcentrifuge CM-50 (ELMI, USA) prior the NMR measurements.

126    Measurements were done one day after sample preparation. Freshly prepared samples

127    contained 60% heavy water and had pH 6.3-6.1. With time, medium was moderately acidified

128    (to pH~5.0) due to the lactate formation. Although sample preparation was carried out

129    carefully and thoroughly, no special steps were taken to ensure sample sterility.

130        Antibiotics gentomicin (Asparin, Germany) and amphotolecin B (Sigma) used for

131    prevention of microbial contamination at the cell culture (Soloviev*a et al*., 2008) were

132    dissolved in 2 ml of D2O to ensure final concentrations of 40 µg/ml (gentamicin) and 2

133    µg/ml (amphotolecin B) in the mitochondria suspension samples and of 5 µg/ml (gentamicin)

134    and 0.4 µg/ml (amphotolecin B) in the liver homogenate samples. Sodium azide

135    concentration was kept at the level of 0.2%.

136        NMR spectrometer AVANCE 600 (BRUKER) with the operating frequency 600.13 MHz

137    was used in the experiments. ^{1}H-NMR spectra were measured using the spectral width of

138    8000 Hz, 90° pulse of 11 microseconds, and temperature of 298 K. As a rule, 128

139    accumulations were sufficient to obtain good signal to noise ratio. The NMR spectra were

140    obtained using the pulse sequences "WATERGATE" and "ZPRG" with the relaxation delay

141    from 1 to 3 s. The heavy water content was determined using the "ZG" pulse sequence. Here,

142    NMR spectra of the samples with known ratios of light and heavy water were measured with

143    the relaxation delay of 10 s. These spectra were analyzed to measure the spectral intensities

144    of water signal which then were used to make a calibration plot. Heavy water content in all

145    working samples was evaluated using this calibration plot.

146        ^{2}H-NMR spectra were measured using the 20W field stabilizer at the frequency of 92.12

147    MHz, 90°-impulse length of 150 microseconds, a spectrum width of 8000 Hz and 500-1000

148    accumulations. All the measurements were done at 298 K inside the sensor. The Fourier

149    transformation was carried out at doubled point array using the simple exponential

150    multiplication with the constant of 1.0 Hz and 0.2 Hz for the proton and deuterium spectra,

151    respectively.

152

## Results and discussion

**Mitochondria from rat liver**

155    It is believed that the isolated from the rat liver mitochondria preserve their functional

156  activity *in vitro* for 1-3 hrs after isolation (Belosludtse*v et al*., 2009). The proton NMR

157  spectrum of the suspension of mitochondria isolated using the heavy water-based protocol

158  that was collected during this initial time of the sustained mitochondrial activity is shown in

159  Figure 1A. This spectrum is dominated by the rather broad signals typical of the intracellular

160  organic molecules. Note that narrow and very intensive signals correspond in a region from

161  4.7 to 3.5 ppm to sucrose, which is present in the extracellular medium due to the

162  peculiarities of the isolation protocols (Figure 1A) (Belosludtse*v et al*., 2009). In the

163  absorption region of the aliphatic protons (from 3.0 to 0.5 ppm), the major components are

164  broad signals corresponding to the mitochondrial membranes. After 10-12 hrs of incubation,

165  some sharp signals start to appear (see Figure 1B). These signals correspond to the organic

166  molecules extruded from the mitochondria to medium. With time, the amplitudes and number

167  of these sharp signals increase, whereas the amplitudes of broad signals proportionally

168  decrease. At this moment, spectrum contains signals of free amino acids and other organic

169  components, which are commonly detected in other biological fluids and aqueous extracts

170  from various plant and animal tissues. Figure 1C shows typical 1H-NMR spectrum of the

171  aqueous extracts of the rat liver homogenate. Spectrum contains sharp signals of free amino

172  acids that coincide with signals detected in all major biological fluids. In fact, ^{1}H-NMR

173  spectra of the biological fluids studied so far are quantitatively similar possessing some

174  fluid/condition-specific qualitative differences. Comparison of Figures 1C and 1B revealed

175  that the majority of sharp signals detected in the ^{1}H-NMR spectrum of the aqueous extract of

176  the rat liver homogenate coincide with those in the ^{1}H-NMR spectrum of the mitochondria. In

177 the $^1$H-NMR spectrum of the aqueous extract of the rat liver homogenate, the most

178 characteristic signals with highest intensities correspond to glucose. During the observation

179 for 3-5 days, proton spectra of the aqueous extracts did not change neither qualitatively nor

180 quantitatively.

181      Interestingly, signals in the $^2$H-NMR spectrum with the satisfactory signal-to-noise ratio

182 that can be used for the qualitative measurements start to appear only after the incubation for

183 about 20 hrs, although some signals are clearly detectable at earlier time points. On a second

184 day, the $^2$H-NMR spectrum is completely formed, and subsequent incubation results in the

185 increase of amplitudes of already existing signals. Figure 2 represents this process by

186 showing normalized integral intensities measured in the range of 3.6-0.0 ppm of proton

187 spectra (black circles) or in the range of 4.2-0.0 ppm of $^2$H-NMR spectra. The increase in the

188 amplitudes of sharp signals in the proton spectra is related to the gradual release of the

189 intramitochondrial organic compounds resulted from the destruction of mitochondrial

190 membranes.

191      During the first 27 hrs after isolation of mitochondria, the kinetics of the formation of

192 proton- and deuterium-containing metabolites are similar due to the insignificant amounts of

193 the low molecular mass (LMM) compounds released from the destroyed mitochondria. These

194 LMM compounds serve as substrates for the metabolism of the contaminating

195 microorganisms and for the residual enzymatic activity of the mitochondrial proteins either

196 released to the medium from the destroyed mitochondria or still located inside the damaged

197 mitochondria. At longer incubation times, kinetic parameters of the observed processes

198 become more and more different. This reflects the existence of an active metabolic

199 conversion of the released substrates by microorganisms and by the residual enzymatic

200 activity of mitochondria. Importantly, the proton spectra of mitochondria do not qualitatively

201  change with time; i.e., no new signals appear and no old signals completely disappear. The

202  sharp increase in the intensity of signals in the 1H-NMR spectra at the beginning of the

203  second day is associated with the massive death of mitochondria. Exponentially slowing, this

204  process continues for some 50 hours. A plateau and subsequent small increase in the vicinity

205  of 50 hours are determined either by the death of the least sensitive cells or by the 'switching

206  on' of some other degradation mechanisms. The monotonous increase in the signal intensity

207  of the $^2$H-NMR spectra is associated with the enzymatic activity and the microbial

208  metabolism. On average, the integral intensities of the $^2$H-NMR spectra are about 1.3-times

209  lower than the amplitudes of peaks in the proton spectra.

210  Figures 3A and 3B represent a pair of typical $^2$H-NMR spectra measured for two

211  mitochondrial isolates randomly selected from a dozen of independent isolation performed

212  during a year using different isolation protocols (sucrose-based and mannitol-sucrose-based),

213  on the basis of $D_2O$ and $H_2O$, respectively. All the recorded spectra possess close similarity to

214  each other, being mostly different in relative intensities of several peaks. Figure 3 represents

215  signal assignments based on the comparison of chemical shifts with proton spectra of known

216  metabolites from various biological fluids. These assignments took into account the presence

217  of the isotope shift and were performed using a large set of 2H-NMR spectra of samples

218  prepared from various plant and animal sources. The major difference between spectra shown

219  in Figures 3A and 3B is in lesser amounts of ethanol and acetate in mitochondrial

220  preparations utilizing heavy water. Furthermore, in all the cases of heavy water-based

221  isolations, the rightmost signal corresponding to isotopic variant of acetate ($-CD_3$) was

222  always higher than the middle signal corresponding to $-CHD_2$, since the heavy water content

223  in these samples was ~85%, whereas in light water-based isolations with concomitant

224  addition of $D_2O$, the heavy water content was at the level of 35-40%. The presence of signals

225    corresponding to ethanol, acetate and formate at 8.43 ppm (not shown) is the reflection of the

226    microbial contamination of the isolated mitochondria.

227          Figure 3C represents a typical $^2$H-spectrum of the aqueous extract of liver homogenate.

228    This spectrum, being corrected for the differences in intensity of some signals, resembles

229    spectrum of the mitochondria isolates. However, since this spectrum possesses signals

230    corresponding to ethanol, formate, and acetate, one can suggest that these samples were

231    contaminated by microorgansims. To identify signals corresponding to the products of the

232    microbial metabolism, some broad-spectrum antibiotics or sodium azide were added during

233    the sample preparation. Similar to antibiotics, sodium azide (low concentration of which are

234    used as preservative in the food industry) possess antimicrobial activities. Sodium azide

235    predominantly affects Gram-negative bacteria, suppressing their growth and development.

236    The application of both bactericides had similar outputs, and the resulting $^2$H-NMR spectra of

237    the aqueous extract of liver homogenates treated with antibiotics and sodium azide were

238    identical.

239          Figure 3D represents one of the spectra for bactericide-treated sample and shows the lack

240    of signals corresponding to ethanol, formate, and acetate, supporting their bacterial origin.

241    Therefore, resulting spectra contain only signals corresponding to the compounds produced

242    by mitochondrial enzymes under the proton-deuterium exchange conditions. The liver

243    extracts contain both substrates and ferments that participate in the enzymatic reactions

244    uncontrolled by the decomposed cells. The corresponding $^2$H-NMR spectra contain alanine,

245    glycine, and lactate (Figure 3D), with alanine being the dominating component. It is known

246    that alanine accounts for ~30% of all amino acids delivered to the liver. This explains

247    relatively high concentrations of alanine in the liver preparations (see Figure 2C). In the liver,

248  alanine is converted to pyruvate, which is subsequently used for the glucose synthesis

249  (Malaiss*e et al.*, 1996; Burell*e et al.*, 2000).

250      In our experiments, the samples were prepared by the mechanical homogenization of rat

251  livers. Therefore, the resulting homogenate contains some surviving cells that remain

252  functional and continue function more-or-less normally, at least for some time. Therefore,

253  these preparations can be considered as a model of severe tissue damage. Survived cells

254  continue to express proteins and possess metabolic processes supporting cell life activity.

255  Under the oxygen deficiency conditions of our experiments, the only available pathway for

256  energy generation in a cell is anaerobic glycolysis. However, the last stage of this pathway is

257  likely to be failed as evidenced by the lack of the increase in the lactate signal in the

258  corresponding 1H-NMR spectra (see Figure 1C).

259      Pyruvate produced during glycolysis is converted to the alanine via the transamination

260  reaction. This reaction together with the reversed transformation of alanine to pyruvate is

261  catalyzed by the alanine transaminase also known as alanine aminotransferase (Dolle, 2000;

262  Yan*g et al.*, 2009). The activity of this enzyme combined with the protein degradation and

263  membrane decomposition, together with the presence of some free alanine inside the cells

264  give likely explanation for the moderate increase in the alanine signal in the spectra of rat

265  liver homogenates during their long-term observation. The presence of deuterium in the C$\alpha$

266  position and in the methyl groups of alanine supports the enzymatic origin of alanine's

267  hydrocarbon skeleton (see Figure 4).

268      Figure 5 represents the $^2$H-NMR spectra of mitochondria in samples containing

269  antibiotics. Comparison of spectra measured at different time points after the sample

270  preparation indicates the presence of some kinetic processes. Figure 5C shows signals

271  accumulated during the first 8 hrs of sample incubation. The most intensive signal here is a

272    signal from the glycine deuterons followed by a less intensive signal of deuterated alanine.

273    Furthermore, spectrum contains signals corresponding to the proton-deuterium exchange at

274    nitrogens of urea (5.7 ppm), and side chains of glutamine (~7.6 ppm) or asparagine (~6.9

275    ppm) or both residues (~7.6 ppm and ~6.9 ppm). These signals significantly increase after

276    one day incubation (see Figure 5C) but did not change much during the more prolonged

277    incubation.

278      To the sixth day, spectrum undergoes further changes, and signals of lactate and formic

279    acid appear, whereas signals corresponding to the nitrogen disappear. These changes reflect

280    starting bacterial activity leading to the nitrogen utilization and appearance of own

281    metabolites. Concentrations and ratios of antibiotics were carefully selected to suppress the

282    bacterial activity and not to produce additional damage of the liver cells. In these settings, the

283    bacterial activity was sufficiently suppressed, since in the absence of antibiotics, signals

284    corresponding to lactate and ethanol were easily detectable already after 2-3 days (see Figure

285    3).

286      The major glycine biosynthetic pathway in a cell is the one catalyzed by the serine

287    hydroxymethyltransferase, an enzyme that plays an important role in cellular one-carbon

288    pathways by catalyzing the reversible, simultaneous conversions of L-serine to glycine

289    (retro-aldol cleavage) and tetrahydrofolate to 5,10-methylenetetrahydrofolate (hydrolysis)

290    (Appaji Ra*o et al.*, 2003; Scheer, Mackey & Gregory, 2005; Berdyshe*v et al.*, 2011). Figure 4

291    shows that serine is synthesized in a cell from the 3-phosphoglycerate, which is one of the

292    intermediates of the glycolysis, and glutamine, which serves as the source of amine. Serine is

293    subsequently used for the protein biosynthesis and for the synthesis of phosphatidylserine that

294    constitutes typically ~15% of all membrane phospholipids. The transfer of the serine methyl

295  group to tetrahydrofolate in the presence of heavy water can be accompanied by the

296  deuteration of the $CH_2$-group of the newly synthesized glycine.

297  Our study revealed that high-resolution $^2$H-NMR spectroscopy can be successfully used

298  in metabolomics studies. Furthermore, the strategic use of antibiotics helps discriminating

299  microbial activity from enzymatic cellular processes. The major products of microbial

300  activity are organic acids, such as formate, acetate, lactate, propionate (seeing in spectra of

301  homogenates of heart muscle) and ethanol. It is important to note here that our data suggest

302  that ethanol can originate not only from the classical alcoholic fermentation but can be

303  generated via some other processes. This conclusion is based on the uneven intensities of

304  $-CD_2-$ and $-CD_3$ deuterons reproducible detected in our experiments, whereas these signals

305  would have comparable intensities if ethanol would be exclusively generated via the

306  alcoholic fermentation pathway due to the more efficient deuteration of methylene group

307  (Kutyshenko & Iurkevich, 2000).

308  The major substrates for the ethanol formation are pyruvic acid and acetaldehyde. There

309  are several biosynthetic pathways for the production of these compounds in the organism, and

310  pyruvate and acetaldehyde can be generated from glucose (as a result of glycolysis), pentoses

311  (via pentose phosphate pathway) or from some amino acids (e.g., due to the catabolism of

312  alanine and threonione) (see Figure 4). Therefore, the ethanol formation is likely a reflection

313  of the successful development of the contaminating bacterial and fungal microbiomes. Based

314  on the characteristic patterns of the hydrogen substitution by deuterium, we hypothesize that

315  the significant part of the endogenous ethanol in our settings is synthesized from the

316  deaminated amino acids (see Figure 4). For example, during the processes of alanine

317  transamidation and threonine degradation, the resulting terminal $CH_3$-groups of pyruvate and

318  acetaldehyde are efficiently deuterated. The subsequent fermentation of pyruvate to ethanol

319    in the presence of heavy water may be accompanied by the deuteration of ethanol's

320    $-CH_2$-group. Resulting $^2$H-NMR spectra of ethanol derived from these intermediates suggest

321    almost proportional saturation of $CH_3$- and $-CH_2$-groups, in sharp contrast to the

322    disproportional saturation of these groups in ethanol molecules produced via the glucose

323    fermentation.

324

## 325    Acknowledgements

330 **References**

331 Appaji Rao, N., Ambili, M., Jala, V.R., Subramanya, H.S., Savithri, H.S. 2003.
332         Structure-function relationship in serine hydroxymethyltransferase. *Biochim Biophys*
333         *Acta* 1647: 24-29.
334 Belosludtsev, K.N., Saris, N.E., Belosludtseva, N.V., Trudovishnikov, A.S., Lukyanova, L.D.,
335         Mironova, G.D. 2009. Physiological aspects of the mitochondrial cyclosporin
336         A-insensitive palmitate/Ca2+-induced pore: tissue specificity, age profile and
337         dependence on the animal's adaptation to hypoxia. *J Bioenerg Biomembr* 41: 395-401.
338 Berdyshev, A.G., Gulaia, A.A., Chumak, A.A., Kindruk, N.L. 2011. [Effect of
339         N-stearoylethanolamine on free amino acid levels in rat plasma and liver with burn].
340         *Biomed Khim* 57: 446-454.
341 Budantsev, A.Y., Uversky, V.N., Kutyshenko, V.P. 2010. Analysis of the metabolites in apical
342         area of Allium cepa roots by high resolution NMR spectroscopy method. *Protein Pept*
343         *Lett* 17: 86-91.
344 Burelle, Y., Fillipi, C., Peronnet, F., Leverve, X. 2000. Mechanisms of increased
345         gluconeogenesis from alanine in rat isolated hepatocytes after endurance training. *Am*
346         *J Physiol Endocrinol Metab* 278: E35-42.
347 Dolle, A. 2000. Metabolism of D- and L-[(13)C]alanine in rat liver detected by (1)H and
348         (13)C NMR spectroscopy in vivo and in vitro. *NMR Biomed* 13: 72-81.
349 Emsley, J.W., Feeney, J., Sutcliffe, L.H. 1966. *High resolution nuclear magnetic resonance*
350         *spectroscopy* Pergamon Press, Oxford.
351 Ewy, C.S., Ackerman, J.J., Balaban, R.S. 1988. Deuterium NMR cerebral imaging in situ.
352         *Magn Reson Med* 8: 35-44.
353 Holmes, E., Wilson, I.D., Nicholson, J.K. 2008. Metabolic phenotyping in health and disease.
354         *Cell* 134: 714-717.
355 Human, Microbiom, Project, Consortium 2012a. A framework for human microbiome
356         research. *Nature* 486: 215-221.
357 Human, Microbiom, Project, Consortium 2012b. Structure, function and diversity of the
358         healthy human microbiome. *Nature* 486: 207-214.
359 Kushner, D.J., Baker, A., Dunstall, T.G. 1999. Pharmacological uses and perspectives of
360         heavy water and deuterated compounds. *Can J Physiol Pharmacol* 77: 79-88.
361 Kutyshenko, V.P., Iurkevich, D.I. 2000. [Identification of partially deuterated exometabolites
362         during culture of tea fungi in heavy water]. *Biofizika* 45: 1096-1101.
363 Kutyshenko, V.P., Sviridova-Chailakhyan, T.A., Molochkov, N.V., Chailakhyan, L.M. 2008a.
364         A study of the organic compound composition of mouse male reproductive organs by
365         high resolution NMR. *Dokl Biochem Biophys* 420: 99-104.
366 Kutyshenko, V.P., Sviridova-Chailakhyan, T.A., Stepanov, A.A., Chailakhyan, L.M. 2008b. A
367         study of the composition of organic substances in early mouse embryos by proton
368         magnetic resonance. *Dokl Biochem Biophys* 422: 270-273.
369 Kutyshenko, V.P., Sviridova-Chailakhyan, T.A., Stepanov, A.A., Tsoi, N.G., Chailakhyan,
370         L.M. 2007. A study of the composition of organic compounds in mouse reproductive
371         organs at early pregnancy stages by proton magnetic resonance. *Dokl Biochem*
372         *Biophys* 414: 109-112.
373 Maher, A.D., Crockford, D., Toft, H., Malmodin, D., Faber, J.H., McCarthy, M.I., Barrett, A.,
374         Allen, M., Walker, M., Holmes, E., Lindon, J.C., Nicholson, J.K. 2008. Optimization
375         of human plasma 1H NMR spectroscopic data processing for high-throughput
376         metabolic phenotyping studies and detection of insulin resistance related to type 2
377         diabetes. *Anal Chem* 80: 7354-7362.

378  Malaisse, W.J., Zhang, T.M., Verbruggen, I., Willem, R. 1996. D-glucose generation from
379      [2-13C]pyruvate in rat hepatocytes: implications in terms of enzyme-to-enzyme
380      channelling. *Arch Biochem Biophys* 332: 341-351.
381  Molchanov, M.V., Kutyshenko, V.P., Budantsev, A.Y., Ivanitsky, G.R. 2012. From fragments
382      to morphogenesis: NMR spectroscopy of metabolites in the apex of the roots of onion.
383      *Dokl Biochem Biophys* 442: 52-56.
384  Nicholson, J.K., Lindon, J.C. 2008. Systems biology: Metabonomics. *Nature* 455:
385      1054-1056.
386  Popova, I.Y., Sinelnikova, V.V., Kitchigina, V.F. 2008. Disturbance of the correlation between
387      hippocampal and septal EEGs during epileptogenesis. *Neurosci Lett* 442: 228-233.
388  Riabichenko, E.V., Bondarenko, V.M. 2007. [Role of gut bacterial autoflora and its
389      endotoxins in human pathology]. *Zh Mikrobiol Epidemiol Immunobiol*: 103-111.
390  Scheer, J.B., Mackey, A.D., Gregory, J.F., 3rd 2005. Activities of hepatic cytosolic and
391      mitochondrial forms of serine hydroxymethyltransferase and hepatic glycine
392      concentration are affected by vitamin B-6 intake in rats. *J Nutr* 135: 233-238.
393  Solovieva, M.E., Solovyev, V.V., Kudryavtsev, A.A., Trizna, Y.A., Akatov, V.S. 2008. Vitamin
394      B12b enhances the cytotoxicity of dithiothreitol. *Free Radic Biol Med* 44: 1846-1856.
395  Tancrede, C. 1992. Role of human microflora in health and disease. *Eur J Clin Microbiol*
396      *Infect Dis* 11: 1012-1015.
397  Yang, R.Z., Park, S., Reagan, W.J., Goldstein, R., Zhong, S., Lawton, M., Rajamohan, F.,
398      Qian, K., Liu, L., Gong, D.W. 2009. Alanine aminotransferase isoenzymes: molecular
399      cloning and quantitative analysis of tissue expression in rats and serum elevation in
400      liver toxicity. *Hepatology* 49: 598-607.
401  Yu, L.C., Wang, J.T., Wei, S.C., Ni, Y.H. 2012. Host-microbial interactions and regulation of
402      intestinal epithelial barrier function: From physiology to pathology. *World J*
403      *Gastrointest Pathophysiol* 3: 27-43.
404
405

406  **Figure legends**

407  **Figure 1**. $^1$H-NMR spectra of biological fluids. **A**. Suspension of mitochondria isolated from

408  rat liver. Measurements were done immediately after the mitochondra isolation. **B**.

409  Suspension of mitochondria isolated from rat liver. Measurements were done one day after

410  the isolation. **C**. Aqueous extract of the rat liver homogenate.

411

412  **Figure 2**. Time courses of changes in the integral intensities of the aliphatic signals in the

413  $^1$H-NMR (black circles) and $^2$H-NMR spectra (open circles) of the suspension of

414  mitochondria isolated from rat liver using $D_2O$-based protocol.

415

416  **Figure 3**. $^2$H-NMR spectra of biological fluids. **A**. mitochondria suspension isolated using

417  $H_2O$-based protocol. **B**. mitochondria suspension isolated using $D_2O$-based protocol. **C**.

418  Aqueous extract of the rat liver homogenate without sodium azide. **D**. Aqueous extract of the

419  rat liver homogenate with sodium azide added.

420

421  **Figure 4**. Various pathways of the metabolite conversion in cytosol and mitochondria of rat

422  liver at which hydrocarbon skeleton of resulting compounds can be deuterated. Conversion of

423  the hydrocarbon skeleton of metabolytes to ethanol at long incubation times is determined by

424  the contaminating microorganisms.

425

426  **Figure 5**. Time course of changes in the $^2$H-NMR spectra of mitochondria suspension

427  samples with added antibiotics. **A**. Spectrum is taken on sixth day after the sample

428  preparation. **B**. Spectrum is taken on second day after the sample preparation. **C**. Spectrum is

429  taken 8 hours after the sample preparation. All samples contained low concentrations of

430  antibiotics at the levels typically used in cell cultures.

# Figure 1

Figure 1

[1] H-NMR spectra of biological fluids. **A**. mitochondrion isolated from rat liver. Measurements were done immediately after mitochondrion isolation. **B**. mitochondrion isolated from rat liver. Measurements were done one day after isolation. **C**. Aqueous extract of the rat liver homogenate.
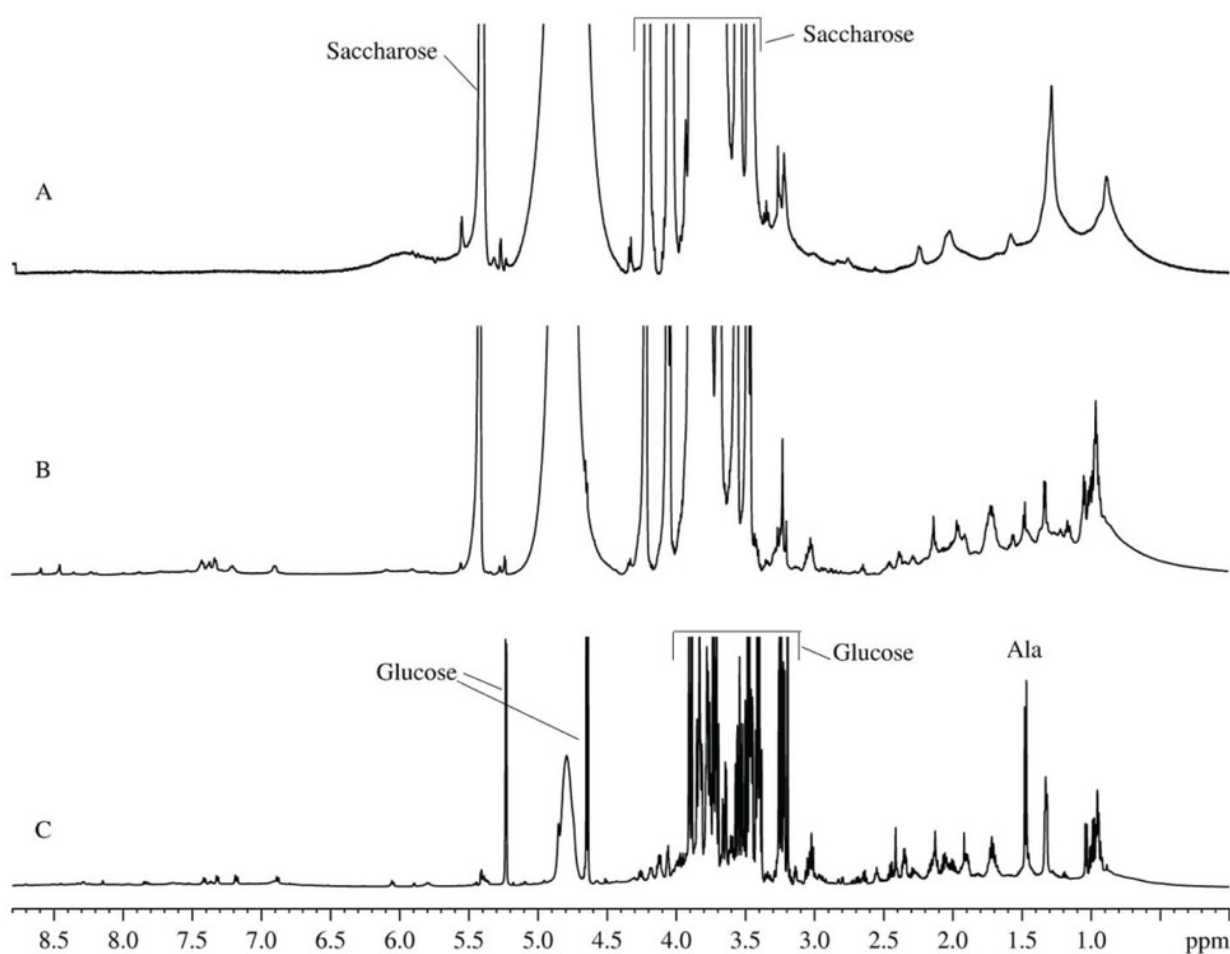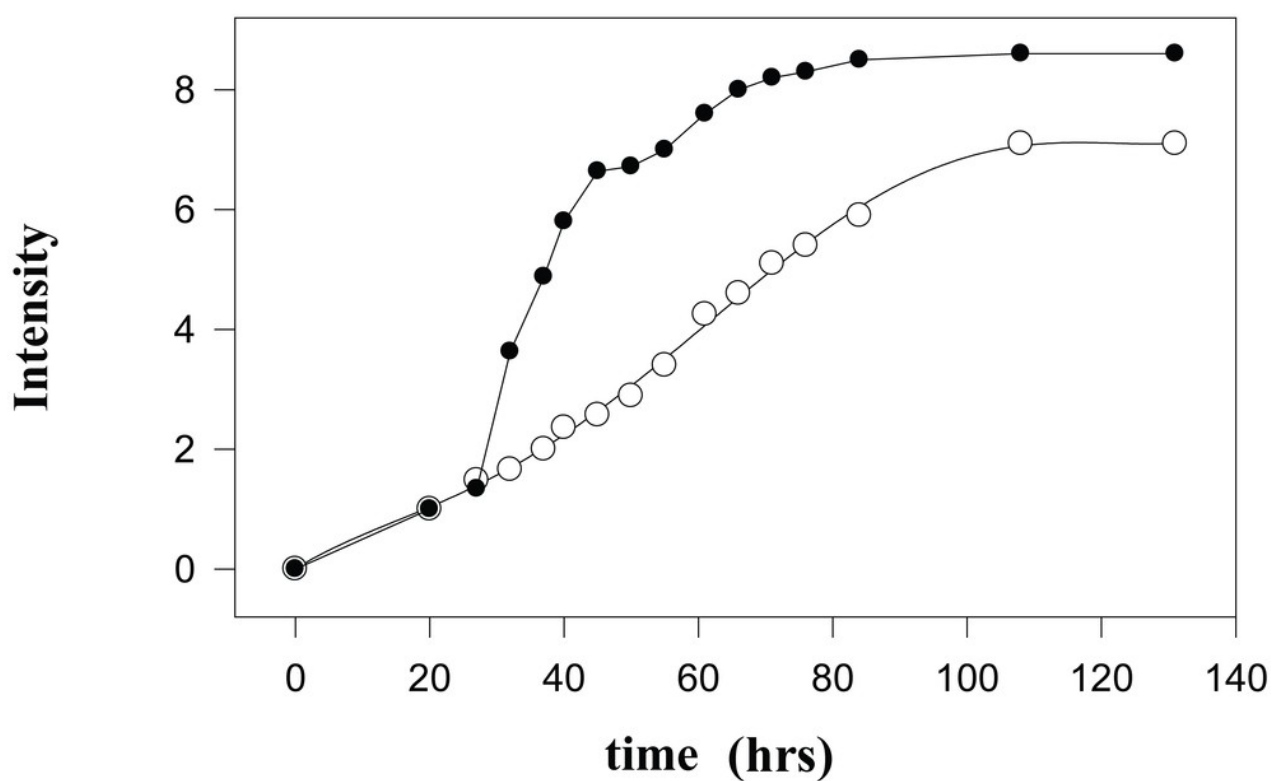
# Figure 2

Figure 2

Time courses of changes in the integral intensities of the aliphatic part of $^1$H-NMR (black circles) and $^2$H-NMR spectra (open circles).

# Figure 3

Figure 3

[2] H-NMR spectra of biological fluids. **A**. mitochondrion isolated using $D_2O$-based protocol. **B**. mitochondrion isolated using $D_2O$-based protocol. **C**. Aqueous extract of the rat liver homogenate. **D**. Aqueous extract of the rat liver homogenate with sodium azide added.
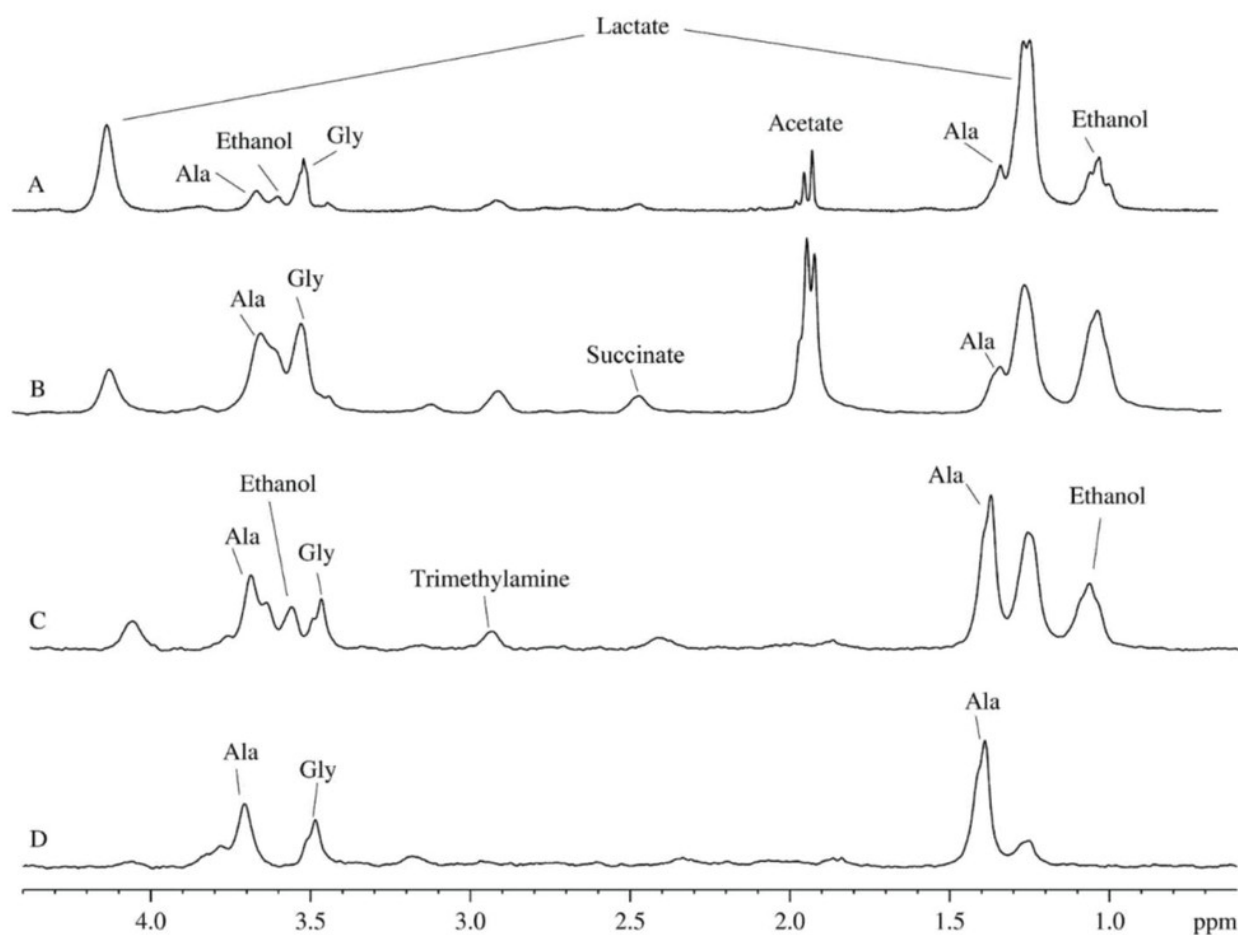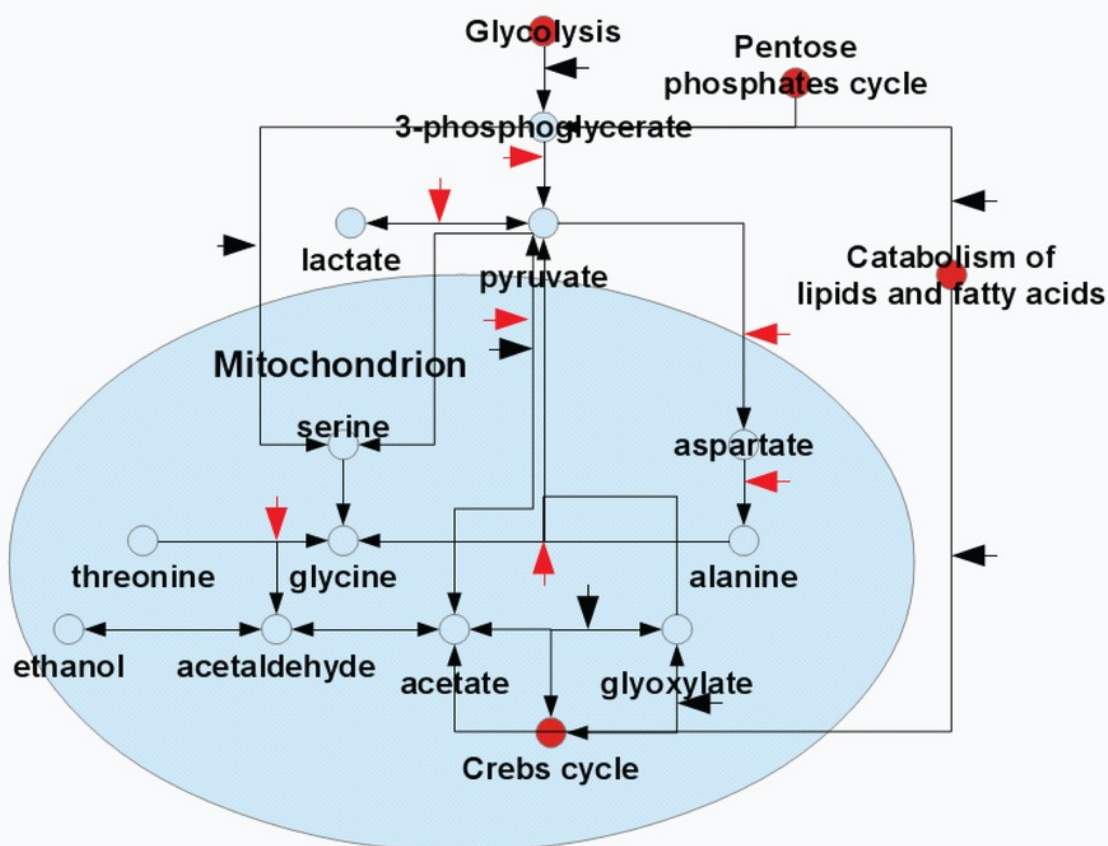
# Figure 4

Figure 4

Various pathways of the metabolite conversion in cytosol and mitochondrion of rat liver at which hydrocarbon skeleton of resulting compounds can be deuterated.

# Figure 5

Figure 5

Time course of changes in the $^2$H-NMR spectra of mitochondrion samples with added antibiotics. A. Spectrum is taken on sixth day after the sample preparation. B. Spectrum is taken on second day after the sample preparation. C. Spectrum is taken 8 hours after the sample preparation.